



Aircraft Engineering and Aerospace Technology

Ring gyroscope sensitive element based on nanoporous alumina

Gennady Gorokh, Yauhen Belahurau, Anna Zakhlebayaeva, Igor Taratyn, Viatcheslav Khatko,

Article information:

To cite this document:

Gennady Gorokh, Yauhen Belahurau, Anna Zakhlebayaeva, Igor Taratyn, Viatcheslav Khatko, (2018) "Ring gyroscope sensitive element based on nanoporous alumina", Aircraft Engineering and Aerospace Technology, Vol. 90 Issue: 1, pp.43-50, <https://doi.org/10.1108/AEAT-01-2015-0026>

Permanent link to this document:

<https://doi.org/10.1108/AEAT-01-2015-0026>

Downloaded on: 07 February 2018, At: 04:49 (PT)

References: this document contains references to 15 other documents.

To copy this document: permissions@emeraldinsight.com

The fulltext of this document has been downloaded 13 times since 2018*

Users who downloaded this article also downloaded:

(2017), "Design practice in the translation traditional and glass cockpit based on General Aviation I-31T aircraft", Aircraft Engineering and Aerospace Technology, Vol. 89 Iss 6 pp. 749-756 <<https://doi.org/10.1108/AEAT-04-2016-0058>>

(2018), "Fatigue based design and life estimation of viscoelastic rotors", Aircraft Engineering and Aerospace Technology, Vol. 90 Iss 1 pp. 96-103 <<https://doi.org/10.1108/AEAT-01-2015-0015>>

Access to this document was granted through an Emerald subscription provided by Token:Eprints:RKDHIJTDJGCJBEZFZE43:

For Authors

If you would like to write for this, or any other Emerald publication, then please use our Emerald for Authors service information about how to choose which publication to write for and submission guidelines are available for all. Please visit www.emeraldinsight.com/authors for more information.

About Emerald www.emeraldinsight.com

Emerald is a global publisher linking research and practice to the benefit of society. The company manages a portfolio of more than 290 journals and over 2,350 books and book series volumes, as well as providing an extensive range of online products and additional customer resources and services.

Emerald is both COUNTER 4 and TRANSFER compliant. The organization is a partner of the Committee on Publication Ethics (COPE) and also works with Portico and the LOCKSS initiative for digital archive preservation.

*Related content and download information correct at time of download.

Ring gyroscope sensitive element based on nanoporous alumina

Gennady Gorokh

Department of Micro- and Nanoelectronics, Belarusian State University of Informatics and Radioelectronics, Minsk, Belarus

Yauhen Belahurau

Department of Micro- and Nanotechnics, Belarusian National Technical University, Minsk, Belarus

Anna Zakhlebayaeva

Department of Micro- and Nanoelectronics, Belarusian State University of Informatics and Radioelectronics, Minsk, Belarus

Igor Taratyn

Department of Micromechanics, Minsk Research Institute of Radiomaterials, Minsk, Belarus, and

Viatcheslav Khatko

Department of Micro- and Nanotechnics, Belarusian National Technical University, Minsk, Belarus

Abstract

Purpose – This paper aims to present new technological approaches of manufacturing of micromechanical gyroscope ring-sensitive element based on the nanoporous anodic alumina instead of traditional silicon technology. Simulation and the operation analyses of such elements have been performed.

Design/methodology/approach – The design of gyroscope represents a sensitive element on a glass substrate; in the center of a ring, there is a permanent magnet in a steel box. The sensitive element is made of profiled nanoporous anodic alumina consisting of an octagonal frame which is connected to a ring in the center with eight N-shaped spokes. The technology of the sensitive element fabrication involves the electrochemical formation of nanoporous anodic alumina substrate given the thickness and porosity and its chemical etching on the element topology. The basic parameters and the operation principle of the nanoporous alumina-sensitive element have been defined by finite element simulation.

Findings – It is shown that the resonance frequencies of the sensitive element change as functions of the alumina porosity. The main parameters of the nanoporous alumina-sensitive element have been compared with parameters of a silicon-sensitive element. Calculations have shown that the mechanical deformations of the von Mises are approximately lower by two times in the nanoporous alumina-sensitive element.

Practical implications – High-precision angular rate measurement will be achieved by reducing mechanical and electrical noises practically to zero through careful designing of a ring magnetoelectric gyroscope

Originality/value – The ring resonator made of nanoporous anodic alumina will allow to increase the threshold of sensitivity and stability of micromechanical gyroscope characteristics owing to the high precision of geometric dimensions, the stability of the elastic properties and the quality factor.

Keywords Finite element method, Gyroscope-sensitive element, Mechanical strain, Modal test, Nanoporous anodic alumina, Ring gyroscope

Paper type Research paper

Nomenclature

Symbols

u = the radial displacement (mm);
 v = the tangential displacement (mm);
 T = kinetic energy (J);
 Q_w, Q_v = the external forces (N);
 ρ = the material density (kg/m^3);
 F = the area of the ring (mm^2);

r = the radius of the ring (mm);
 a_i = the displacement function (–);
 b_i = the time function (–);
 M = the moment of deflection ($\text{N}\cdot\text{m}$);
 I = the moment of inertia ($\text{kg}\cdot\text{m}^2$);
 F_D = the damping force (N);
 F_k = the Coriolis force (N);
 F_c = the centrifugal force (N);
 r_0 = the ring radius in a middle line (mm)
Definitions, Acronyms and Abbreviations;
CAD = computer-aided design;
MMG = micromechanical gyroscope;
NAA = nanoporous anodic alumina; and
SEM = scanning electron microscopy.

The current issue and full text archive of this journal is available on Emerald Insight at: www.emeraldinsight.com/1748-8842.htm



Aircraft Engineering and Aerospace Technology
90/1 (2018) 43–50
© Emerald Publishing Limited [ISSN 1748-8842]
[DOI 10.1108/AEAT-01-2015-0026]

Received 30 January 2015

Revised 10 June 2016

Accepted 14 June 2016

Introduction

Basic elements of mobile objects orientation and navigation microsystems are micromechanical sensors for measuring the angular velocity of the objects (Apostolyuk, 2006). Micromechanical gyroscopes (MMG) are designed to manage various objects of military aerospace and civil applications. The operation of MMG is based on transfer of energy between two vibrational modes of a proof mass owing to the Coriolis effect (Shkel, 2006). A solid-state wave gyroscope can be used to measure the angular velocity of a rotating body based on the inertia effect of the standing wave in two vibration modes of an axisymmetric resonator, which have advantages such as small size, high operation accuracy, low cost, low power consumption, good shock resistance and long life (Matveev *et al.*, 2009; Matthews and Rybak, 1992). These advantages offered by solid-state wave gyroscope have always been of great interest to many researchers, institutes and companies.

Initially a gyroscope basing on a magnetoelectric effect was created by Silicon Sensing Systems using silicon technology (Hopkins, 2001). However, the anisotropy of silicon properties is the cause of dissimilar mechanical properties of MMG elastic elements, and it consequently leads to an error in the measurement of the angular velocity depending on the direction of its action (Martynenko *et al.*, 2010). The use of a material for manufacturing of the sensor having isotropic properties would eliminate these drawbacks and increase the sensitivity of gyroscopes. The nanoporous anodic alumina (NAA) has a unique cellular-porous structure, the vertical pores of which penetrate the oxide from the surface to the base (Surganov and Gorokh, 1993). Whereby the membranes or substrates made of NAA will have isotropic properties, so the aforementioned disadvantages will be avoided (Surganov and Gorokh, 1997). By varying conditions of oxide formation, we can change the structure and mechanics and other properties of the NAA and therefore the substrate characteristics. Very recently the first attempts to combine the anodic alumina with micro-machined silicon technology were made (Khatko *et al.*, 2006), and a porous alumina used as supported substrates for gas sensors has been demonstrated (Gorokh *et al.*, 2014). MMG implemented based on this technology will have a wide dynamic range, and not merely through the design, but also because it is able to control the material mechanical properties.

This paper presents a new approach of the manufacturing process of the sensing element of the ring gyroscope on a substrate of the nanoporous anodic alumina, as well as the simulation and comparison of the parameters of the sensing element of the micromechanical gyroscope of NAA with different porosity and based on silicon technology.

Design concept

MEMS gyroscopic systems are clearly designed with focus on achieving high responsivity, being highly sensitive to angular rate, because the ultimate purpose of this system is angle measurement rather than angular rate measurement. In this section, the design of the ring gyroscope with sensing element based on the nanoporous anodic alumina, and the principle of gyroscope operation is introduced.

Design of the gyroscope

The geometrical model of the ring wave gyroscope is presented in Figure 1(a). The gyroscope has a simple structure comprising a glass substrate, a sensitive element with aluminum metallization and a permanent magnet in a steel box. The sensitive element [shown in Figure 1(b)] is connected to the substrate. The sensitive element consists of an octagonal frame which is connected to a ring in the center with eight N-shaped spokes. The aluminum metallization is situated on the surface of a sensitive element that is made of profiled NAA. The permanent Nd-Fe-B magnet in the steel box is attached to the glass substrate. The overall structure of the ring wave gyroscope is symmetrical about the z (vertical) axis.

Principle of operation

Like all solid-state wave gyroscopes, the principle of the gyroscope operation is based on the inertia effect of the standing wave in two vibration modes of the axisymmetric resonator caused by Coriolis force. The current transfer is realized with aluminum metallization that generates the force, which, in its turn, creates resonance in the system. The ring motion under the effect of the Coriolis force is defined with the voltage generated in the aluminum metallization. Thus, methods of excitation and detection are magnetoelectric. The aluminum metallization is eight equal conductive contours on the sensitive element. Even counter is a sequence: the contact area – the suspend elastic element – the 1/8 ring length – the suspend elastic element – the contact area [Figure 1(b)].

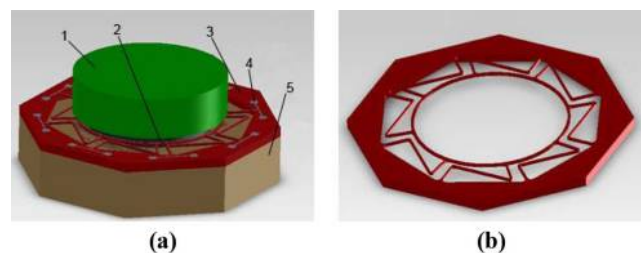
Fabrication of a sensitive element

Fabrication of the ring gyroscope-sensitive element consists of two technological processes – manufacturing process of nanoporous anodic alumina substrate and directly producing the sensing element based on that substrate of a given shape and configuration.

Manufacture of nanoporous anodic alumina substrates

For the manufacture of nanoporous anodic alumina substrates for a ring gyroscope, we used pure aluminum foils of 99.99 per cent purity and 140.0 μm of thickness, cut to dimensions of 60 × 48 mm, as a starting material. Before anodizing, the chemical and mechanical processing of samples was carried out. To remove organic contamination and microscopic

Figure 1 Geometrical model (a) and sensitive element (b) of the ring wave gyroscope



Notes: 1 – steel box; 2 – permanent magnet; 3 – sensitive element; 4 – aluminum-metallization; 5 – glass substrate

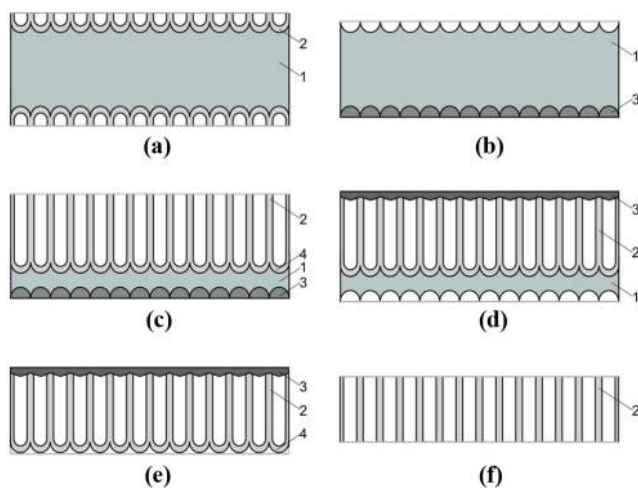
Source: Authors' elaboration

irregularities, the samples were treated sequentially in gasoline for 5 min and in 10 per cent NaOH solution during 15–20 s. Mechanical polishing of the surface was performed by multiple rolling of aluminum samples through polished rollers. To remove the mechanical stresses and impart flatness to the templates, thermo-pressing was performed under the pressure of about 10^7 Pa at 320°C for 1 h. After that treatment, the surface roughness of the aluminum patterns corresponded to a 12 smoothness class.

The experimental setup for aluminum foils' anodization comprised a thermostatically controlled cell with constant mixing electrolyte and a programmed DC power supply controlled by LabVIEW software via a PC and a GPIB interface. The electrical and electrolytic conditions of anodic processing of the aluminum films have been selected to obtain a high-quality porous anodic alumina and make the formation procedure fully compatible with the standard solid-state technologies. A Good Will GPA-60Y15D Laboratory DC Power Supply was used as the anodizing unit.

The polished aluminum foils' anodization was performed in two consequential steps to grow porous anodic alumina with improved pore regularity, enlarged pore outlets and substantially increased surface area at the electrolyte–film interface. Figure 2 shows the main process steps of the NAA substrate preparation. At the first step, the samples were subjected to bilateral electrochemical anodizing in 0.5M oxalic acid electrolyte at a constant voltage of 50 V with a preliminary scan of 10 V/s over a period of 10 min. [Figure 2(a)]. The electrolyte temperature during the process was about 14–16°C.

Figure 2 Main process steps of the NAA substrate preparation



Notes: (a) Formation of porous alumina film on aluminum foil; (b) detaching the alumina film from the residual aluminum substrate and protecting the one side of sample with chemically resistant varnish; (c) main anodizing of aluminum foil; (d) removing varnish layer from aluminum and coating the other side of the substrate with varnish protecting the alumina pores; (e) dissolving the aluminum layer on NAA; (f) dissolving the barrier oxide layer on the bottom side of NAA and removing varnish layer from the surface; 1 – aluminum; 2 – porous anodic alumina; 3 – chemical-resistant varnish; 4 – barrier oxide layer

Sources: Authors' elaboration

The anodizing rate under these conditions was $0.272 \mu\text{m}/\text{min}$. The formed “sacrificial” alumina layers were selectively removed in 20 g/l CrO_3 : 35 ml/l H_3PO_4 solution kept at 60°C (hereafter “selective etchant”) (Wood, 1987). As a result of this process, the aluminum surface is preserved imprints of hexagonal bottoms of the oxide cells [Figure 2(b)]. Then one side of the templates covered by a layer of chemically resistant varnish (thickness of about $15 \mu\text{m}$), which was dried at 20–22°C for 40 min and then in a heat chamber at 90°C for 10 min. The second step, of aluminum foils' anodization with structured surface imprints of oxide cells, was performed in the same electrochemical conditions as the first one. The anodization time was 250 min [Figure 2(c)]. During this time, the other, non-varnished side of aluminum was anodized to a depth of $70 \pm 1 \mu\text{m}$. As a result, the thickness of nanoporous anodic alumina taking into account the influenced by volume growth of oxide (the so-called the value of Pilling–Bedworth ratio: the thickness of the oxide film formed over the depth of the oxidized aluminum metal) (Thompson and Wood, 1983) was about of $100 \pm 1 \mu\text{m}$.

The anodic alumina forming the chemically resistant varnish on the aluminum was removed and the porous alumina surface was covered by another layer of chemically resistant varnish, which was dried in the same conditions as the first one [Figure 2(d)]. The remaining aluminum layer was selectively dissolved away in (1.25 g/l – CuCl_2 ; 840 ml/l – HCl ; 158 ml/l – distilled water) solution (Itaya et al., 1984) kept at 60°C during 25 min [Figure 2(e)]. To remove the copper particles deposited on the anodic alumina surface in the aluminum dissolution process, chemical cleaning was carried out in 90 per cent HNO_3 at 20°C for 1 min. The next step involved dissolving the barrier oxide layer on the bottom side of the NAA in 5 per cent phosphoric acid solution at 50°C for 25 min and removing the varnish layer that was protecting the alumina pore surface [Figure 2(f)]. To enlarge the pores and increase the porosity of anodic alumina, the anodized samples were subjected to pore-widening treatment in 2M H_2SO_4 heated to 50°C and held for 15 min.

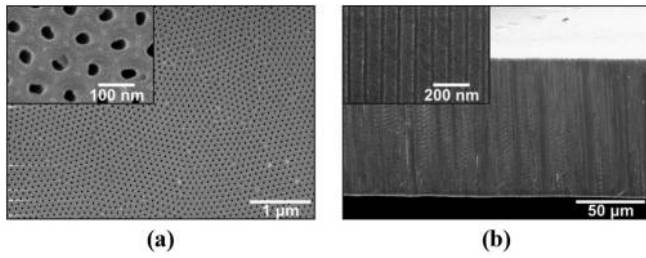
The obtained free layers of NAA of thickness of about $100 \mu\text{m}$ were thoroughly washed in distilled water and dried in an oven at 160°C for 30 min. The morphology and cross sections of the nanoporous anodic alumina substrates observed with a Hitachi S-806 field emission scanning electron microscope are shown in Figure 3.

Fabrication of the sensitive element

The NAA substrates with a thickness of $100 \mu\text{m}$ and a porosity of 15 per cent have been used for fabrication of the sensitive element. The fabrication process of the sensitive element includes fabrication of some parts such as a crystal based on NAA, a frame from NAA and two plates from glass LK-105. For the crystal and frame fabrication, a new technology of the nanoporous alumina micromachining has been developed by the authors of this work.

Fabrication of the crystal consists of following processes. First, a $0.1\text{-}\mu\text{m}$ -thick Pt film was deposited on the substrate surface by means of DC magnetron sputtering of the metallic target. Then a two-layer vanadium–aluminum film system was deposited by vacuum thermal evaporation on both sides of the alumina substrate. The two-layer

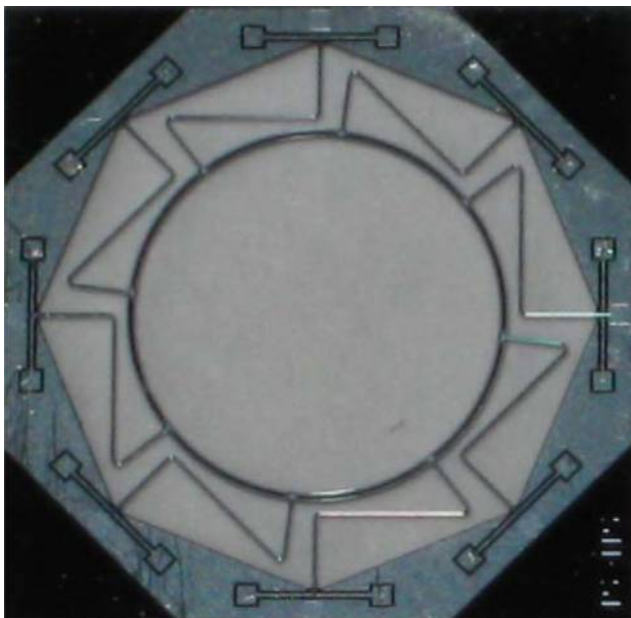
Figure 3 SEM microphotographs of the surface morphology (a) and cross section (b) of the NAA substrate Inserts



Note: SEM images of the surface morphology and cross section of NAA with a high magnification

vanadium–aluminum films were utilized like a technological mask by the formation of the metallization layout. After photolithographic processing, Al and V chemical and Pt ion-beam etching a metallization layout of the crystal was created. The ring spokes and counter of the crystal were made through liquid etching of Al_2O_3 . To this effect, the two-layer vanadium–aluminum film system was deposited again on both sides of the alumina substrate. After photoresist deposition, the ring spokes and counter were lithographically patterned and released by liquid chemical etching of the alumina substrate through the vanadium–aluminum mask. A photoresist and mask removed by chemical etching was the last process step of crystal fabrication. The size of the crystal was $10 \times 10 \text{ mm}^2$, with the distance between vertexes of an interior octagon being 8.8 mm. The thickness of the crystal (counter) was $100 \mu\text{m}$. The outer diameter of the ring was 6.0 mm. The size of the ring and spoke cross section was $100 \times 100 \mu\text{m}^2$. **Figure 4** shows the crystal that is one of the main parts of the sensitive element.

Figure 4 Crystal of wave ring gyroscope-sensitive element



The shape of the frame fit the one of the crystal with the size of $10 \times 10 \text{ mm}^2$, and the distance between the vertexes of the interior octagon was 9.0 mm. The frame of the gyroscope-sensitive element was fabricated using two basic process steps. First, the vanadium and aluminum films were deposited successively on both sides of the new alumina substrate. After photoresist deposition on the top substrate side and photolithographic processing, aluminum and vanadium were chemically etched [**Figure 5(a)**]. Next, an octagon in the NAA frame was made by liquid chemical etching. The photoresist and metallic mask removing by chemical etching was the last process step of the frame fabrication [**Figure 5(b)**].

Assembly of the gyroscope sensitive element from different parts has the following order: the top plate, the frame, the crystal and the down plate. The dimension of the top and down glass plates is $13 \times 13 \text{ mm}^2$; an orifice in the down plate has been manufactured with liquid etching and its diameter is 10 mm. The assembly is performed with low-temperature soldering. The total thickness of crystal and frame in the gyroscope sensitive element could be changed from 100 to $450 \mu\text{m}$.

Simulation and analysis

In this section, the problem for simulating of the sensitive element based on NAA is formulated, and the simulation analysis of the gyroscope parameters is performed.

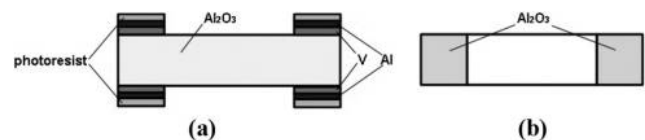
Formulation of the problem

For the fabrication and simulation of devices from the nanoporous anodic oxide of aluminum, a determination of its mechanical properties plays one of the main roles. For determination of NAA mechanical properties we have used the definitions and models obtained in the previous work (Belogurov *et al.*, 2012). In our modelling, we have taken into account that nanoporous anodic alumina is an anisotropic material. For modelling, we have used the NAA elasticity matrix following view:

$$C_{ij} = \begin{pmatrix} c_{11} & c_{12} & c_{13} & c_{14} & 0 & 0 \\ & c_{22} & c_{23} & c_{24} & 0 & 0 \\ & & c_{33} & c_{34} & 0 & 0 \\ & & & c_{44} & 0 & 0 \end{pmatrix}$$

Our modelling has the following objectives: to search for a resonance frequency for optimal work of the sensitive

Figure 5 Process steps of the sensitive element frame fabrication



Notes: (a) Photolithographic processing, chemical etching of aluminum and vanadium; (b) removing photoresist and metallic mask

Source: Authors' elaboration

element and to define mechanical strains, which may arise under the influence of an angular velocity of 2π rad/s and stroke acceleration of $5000g$ with different durations and vibration.

Mathematical framework

The set of Lagrange's equations for the sensitive element is:

$$\begin{aligned} \frac{\partial}{\partial t} \left(\frac{\partial T}{\partial \dot{u}} \right) - \frac{dT}{du} &= Q_u \\ \frac{\partial}{\partial t} \left(\frac{\partial T}{\partial \dot{v}} \right) - \frac{dT}{dv} &= Q_v \end{aligned} \tag{1}$$

where: u and v are the radial and tangential displacements, respectively, T is the kinetic energy and Q_u and Q_v are the external forces.

The kinetic energy of the moving gyroscope-sensitive element can be defined as:

$$T = \frac{\rho F}{2r^2} \int_0^{2\pi} u^2 + v^2 d\theta \tag{2}$$

where: ρ is the material density; F is the area of the ring; and r is the radius of the ring. The calculation scheme is shown in Figure 6.

For the radial movement, we can define as the following trigonometrical range:

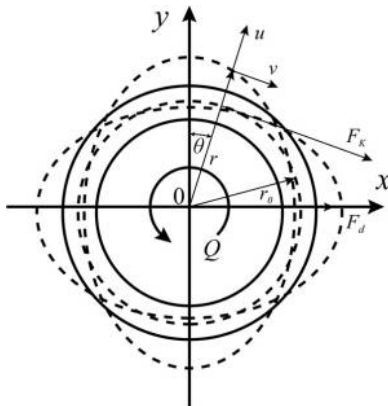
$$u = \sum_{i=1}^{\infty} a_i \cos i\theta + \sum_{i=1}^{\infty} b_i \sin i\theta \tag{3}$$

where: a_i and b_i are the displacement and the time functions, respectively.

For definition of tangential displacement, we have used the Boussinesq's expression for the curvature changing deformed ring:

$$\frac{1}{r + \Delta r} - \frac{1}{r} = -\frac{\partial^2 u}{r^2 \partial \theta^2} - \frac{u}{r^2} \tag{4}$$

Figure 6 The working mode of the sensitive element



From a joint solution of equations (4) and (3) and taking into account the fact that relative extension of the ring is 0, we obtain the following:

$$v = -\sum_{i=1}^{\infty} \frac{a_i \sin i\theta}{i} + \sum_{i=1}^{\infty} \frac{b_i \cos i\theta}{i} \tag{5}$$

Put equations (3) and (5) in equation (2) and then find an expression for determination of the kinetic energy of the motion ring. In this expression, the radial and tangential displacements have been changed on the coefficients of the trigonometrical ranges of equations (3) and (5):

$$T = \frac{\pi r \rho F}{2} \sum_{i=1}^{\infty} \left(1 + \frac{1}{i^2} \right) (a_i^2 + b_i^2) \tag{6}$$

For definition of the external forces in equation (1), the potential energy of bend of the ring is presented in the following expression:

$$V = \frac{1}{2} \int_0^{2\pi} \left(\frac{M^2}{C_{ij} I} - F_{\theta} - F_k - F_c \right) r d\theta \tag{7}$$

where: M is the moment of deflection; I is the moment of inertia; F_{θ} is the damping force; F_k is the Coriolis force; and F_c is the centrifugal force.

Further, the trigonometrical ranges in equations (3) and (5) and the integral expressions:

$$\int_0^{2\pi} \cos m\theta \cos n\theta d\theta = 0, \int_0^{2\pi} \sin m\theta \sin n\theta d\theta = 0,$$

for $m \neq n$ and:

$$\int_0^{2\pi} \cos m\theta \cos n\theta d\theta = 0, \int_0^{2\pi} \cos^2 m\theta = \int_0^{2\pi} \sin^2 m\theta = \pi$$

Have been used for calculation of the potential energy:

$$V = \pi \left[\frac{C_{ij} I}{2r^3} \sum_{i=1}^{\infty} (1 - i^2)^2 (a_i^2 + b_i^2) + \frac{\rho F \Omega r}{i} \sum_{i=1}^{\infty} \dot{a}_i b_i - a_i \dot{b}_i \right] \tag{8}$$

The external forces are connected with the potential energy in the following:

$$Q_u = -\frac{dV}{da_i}, Q_v = -\frac{dV}{db_i} \tag{9}$$

A differential equation relative to the trigonometrical range coefficients follows from the joint solution of equations (1), (4) and (5):

$$\rho F r (1 + i^2) \ddot{a}_i + \frac{C_{ij} I (1 - i^2)}{r_0^3} a_i = \frac{\rho F r b_i}{i} \Omega \tag{10}$$

Where: r_0 is the ring radius in a middle line.

Solution of equation (10) gives an expression for Eigen frequency on the i th mode:

$$\bar{\omega}_i = \frac{1}{2\pi} \sqrt{\frac{C_{ij}I(1-i^2)^2 i^2}{\rho F r_0^4 (1+i^2)}} \quad (11)$$

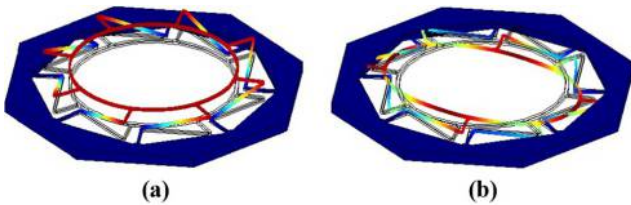
Thus, as a result of analysis of equation (11) used for Eigen frequency calculation of the gyroscope-sensitive element, it can be concluded that the elastic properties, geometrical characteristics and a mode number have an impact on the resonance frequency of the sensitive element, but the angular velocity is not as influential.

Results of modeling and discussion

Figure 7 shows mode shapes of the sensitive element at different frequencies. The porosity and thickness of NAA is 15 per cent and 100 μm, respectively. A working mode of the sensitive element is the sixth mode; therefore, the ring oscillates only in a plane of the sensitive element at the frequency of 16,946 Hz.

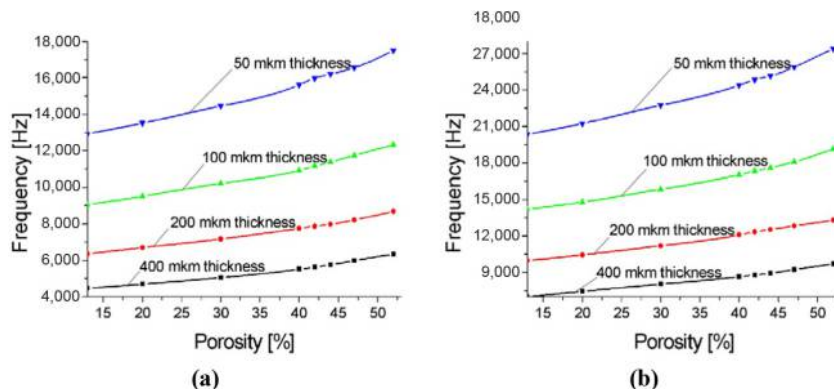
The frequency dependences on the porosity and thickness of the sensitive element were calculated for the first and sixth modes. Figure 8 shows these dependences. It can be seen that the resonance frequency of the working mode changes from 16.5 to 23.0 kHz when the porosity of the sensing element increases from 13 to 52 per cent at the sensing element

Figure 7 The sensitive element shape in the first mode at the frequency of 8,134 Hz (a) and in the sixth mode at the frequency of 16,946 Hz (b)



Source: Authors' elaboration

Figure 8 The frequency dependence on the porosity of the sensitive element for the first (a) and sixth (b) modes for different thicknesses of the NAA substrate



thickness of 100 μm [Figure 8(b), Curve 2]. Decreasing the sensing element thickness increases the frequency value.

It is very important to estimate the level of mechanical deformations that appear in the ring and spokes by rotation of the gyroscope-sensitive element from NAA with an angular velocity of 2π rad/s. Figure 9 shows the result of the modeling. It can be seen that the deformations appearing in the sensitive element by the rotation are very low and cannot be the reason for crack formation and destruction of the ring and spokes.

The sensitive element has been tested on shock acceleration and vibrations as well. The shock acceleration was defined as a single impulse. A value of the impulse is 10,000g and the duration is 5 ms. The vibration frequency is 5 and 40 Hz, and the magnitude is 5g. Time calculation is 1 and 0.125 s accordingly. In Figure 10, the comparison of the silicon-sensitive element and the NAA-sensitive element is shown.

Displacement of the NAA-sensitive element is approximately ten times less. In accordance with this, the strain in the NAA-sensitive element is 10⁻⁵, which is less than the breaking point.

Conclusion

To enhance the sensitivity and measuring accuracy of the angular velocity, it is proposed that nanoporous anodic alumina (NAA) be used as the sensitive element of the micromechanical gyroscope instead of the traditional silicon technology. For this

Figure 9 Simulation of mechanical strain in the sensitive element for angular velocity of 6.28 rad/s

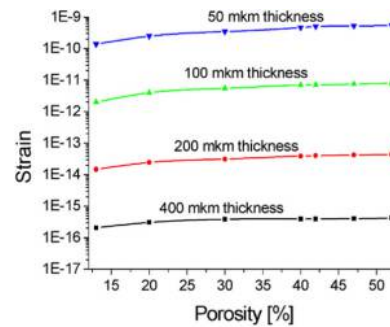
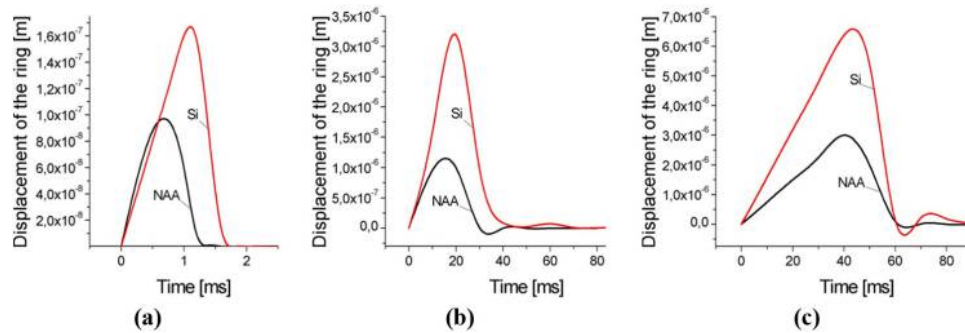


Figure 10 Responses of the NAA- and silicon-sensitive elements on the impulse with length 1 ms (a), with length of 20 ms (b), and with length of 40 ms (c)



purpose, the technology of the nanoporous substrate manufacturing of a given thickness and porosity was developed and the new sensitive element was made from this material. The finite element simulation of a micromechanical gyroscope NAA-sensitive element parameters showed that the sixth mode is the operating mode of the sensitive element and the resonance frequency of the working mode depends on the porosity and thickness of the NAA. The resonance frequency of the working mode increases with an increase in porosity and a decrease in the NAA thickness. At the same time, as a result of the analysis of the gyroscope-sensitive element simulation, it can be concluded that the elastic properties, geometrical characteristics and a mode number have an impact on the resonant frequency of the sensitive element, but the angular velocity is not as influential. The responses' comparison of the NAA- and silicon-sensitive elements on the different impulses showed that the displacement of the NAA-sensitive element is approximately ten times less than that of the sensitive element based on the silicon technology, and the strain in the NAA-sensitive element is 10^{-5} , which is less than the breaking point. Calculations have shown that the mechanical deformations of the von Mises are lower approximately two times in the sensitive element made of the nanoporous anodic alumina.

The working out of the compact micromechanical gyroscopes with the nanostructured ring-sensitive element based on the nanoporous anodic alumina can significantly raise the threshold of sensitivity and the stability of gyroscope characteristics at the expense of precision geometric size and the stability of elastic properties of the sensing element. Currently in the process of preliminary experimental studies of the sensing element in the construction of a micromechanical gyroscope, we are working on finalization and optimization of the ring sensing element design and manufacturing techniques. The next stage of work is a study of key parameters of a ring gyroscope with the nanostructured sensing element.

References

Apostolyuk, V. (2006), "Theory and design of micromechanical vibratory gyroscopes", in Leondes, C.T. (Ed.), *MEMS/NEMS Handbook Techniques and Applications*, Springer, Science + Business Media, Berlin, pp. 173-195.

- Belogurov, E.A., Shukevich, Y.I. and Barkaline, V.V. (2012), "Finite element modelling of thermomechanical properties of nanoporous materials", *Nano and Microsystem Technique*, No. 1, pp. 22-27.
- Gorokh, G.G., Zakhlebayaeva, A.I., Belahurau, Y.A., Khatko, V.V. and Taratyn, I.A. (2014), "Chemical gas sensors on the nanoporous anodic alumina substrate", *Nano and Microsystem Technique*, No. 9, pp. 45-51.
- Hopkins, I. (2001), *Performance and Design of a Silicon Micromachined Gyro*, Silicon Sensing Systems, Application Note, Heidelberg.
- Itaya, K., Sugawara, S., Arai, K. and Saito, S. (1984), "Properties of porous anodic aluminium oxide films as membranes", *Journal of Chemical Engineering of Japan*, Vol. 17 No. 5, pp. 514-520.
- Khatko, V., Gorokh, G., Mozalev, A., Solovei, D., Llobet, E., Vilanova, X. and Correig, X. (2006), "Tungsten trioxide sensing layers on highly ordered nanoporous alumina template", *Sensors and Actuators B: Chemical*, Vol. 118 Nos 1/2, pp. 255-262.
- Martynenko, Y.G., Merkuriev, I.V. and Podalkov, V.V. (2010), "Dynamics of a ring micromechanical gyroscope in the forced-oscillation mode", *Gyroscopy and Navigation*, Vol. 1 No. 1, pp. 43-51.
- Matthews, A. and Rybak, F.J. (1992), "Comparison of hemispherical resonator gyro and optical gyros", *IEEE Aerospace and Electronic Systems Magazine*, Vol. 7 No. 5, pp. 40-45.
- Matveev, V.A., Basarab, M.A. and Alekin, A.V. (2009), *Design of the Solid State Wave Gyro*, National Defence Industry Press, Beijing.
- Shkel, A.M. (2006), "Type I and type II micromachined vibratory gyroscopes", *Proceedings of Position, Location, and Navigation Symposium a Meeting held in San Diego, California, IEEE/ION, San Diego, CA*, pp. 586-593.
- Surganov, V. and Gorokh, G. (1993), "Anodic-oxide cellular structure formation on aluminium films in tartaric acid electrolyte", *Materials Letters*, Vol. 17 Nos 3/4, pp. 121-124.
- Surganov, V. and Gorokh, G. (1997), "Nanoporous aluminum anodic oxide membrane", in Borisenko, V.E. (Ed.), *Physics, Chemistry and Application of Nanostructures: Reviews and Short Notes to Nanomeeting-1997*, World Scientific, Singapore, pp. 306-308.

- Thompson, G.E. and Wood, G.C. (1983), "Anodic films on aluminium", in Scully, J.C. (Ed.), *Corrosion: Aqueous Processes and Passive Films, Vol. 23 of Treatise on Material Science and Technology*, Academic Press, New York, pp. 205-329.
- Wood, G.C. (1987), "Porous anodic films on aluminium", in Diggle, J.W. (Ed.), *Oxides and Oxide Films*, Vol. 2, Marcell Dekker, New York, NY, p. 41.

Further reading

- Apostolyuk, V.A., Logeeswaran, V.J. and Tay, F.E.H. (2002), "Efficient design of micromechanical gyroscopes", *Journal of Micromechanics and Microengineering*, Vol. 12 No. 6, pp. 948-954.

Corresponding author

Gennady Gorokh can be contacted at: gorokh@bsuir.by

For instructions on how to order reprints of this article, please visit our website:

www.emeraldgroupublishing.com/licensing/reprints.htm

Or contact us for further details: permissions@emeraldinsight.com